submitted to *Geophys. J. Int.*

Ratio-to-Moving-Average Seismograms: A Strategy for Improving Correlation Detector Performance

Steven J. Gibbons, Frode Ringdal and Tormod Kværna

NORSAR, P.O. Box 53, 2027 Kjeller, Norway, E-mail: steven@norsar.no

SUMMARY

Correlation detectors are becoming a standard method for identifying seismic signals from repeating sources. These highly sensitive, source-specific, detectors frequently facilitate a reduction in the detection threshold by around an order of magnitude. Detections are typically declared when the value of the correlation coefficient (CC), or a related statistic, exceeds significantly some measure of the variability of values over a longer time window. The performance of correlation detectors is often compromised by the presence of short duration, high amplitude, signals which influence excessively the value of the CC. We suggest replacing the original seismograms with waveforms in which the value of each sample is replaced by the ratio of that value to a centered moving average of absolute values of the original waveform. These ratio-to-moving-average (RMA) seismograms are relatively featureless over long time intervals, but resemble greatly the original waveforms over short time-windows and hence still capture the characteristic seismic fingerprint of a given source. We demonstrate a correlation detection calculation which fails due to the presence of a high amplitude signal interfering with part of the correlation window, but which succeeds when RMA-seismograms are used due to the diminished influence of the interfering signal. We also demonstrate an example from an aftershock sequence where the CC traces are heavily modulated due to the high dynamic range of the original waveforms. This makes the setting of detection thresholds difficult and re-

sults in multiple peaks which do not correspond to events in the vicinity of the master event. Repeating the calculation using RMA-seismograms results in CC traces with a more well-defined detection threshold and most of the spurious detections are lost. The ability to set lower detection thresholds without increasing greatly the number of false alarms facilitates the robust detection of lower magnitude events.

1 INTRODUCTION

The detection of signals using waveform correlation is rapidly becoming a standard method for identifying signals from seismic events from source regions with repeating seismicity. The realization that seismic events within very close proximity of each other produce highly characteristic signals on any given receiver (a kind of seismic "fingerprint", e.g. Geller & Mueller 1980) has led to the realization that correlation (or matched-filter) detectors can constitute highly sensitive detectors for low amplitude signals in situations where so-called master events are available to provide signal templates. Correlators lie at the extreme of the suite of seismic signal detectors for which the form of a signal is known exactly. At the opposite extreme, at which we know nothing about the signal waveform, the most typical procedures detect increases in signal amplitude (e.g. Allen 1978, 1982; Withers et al. 1998) with the most common trigger being the signal-to-noise-ratio (SNR) defined as the ratio between a short-term-average (STA) and a long-term-average (LTA). Between these two extremes, a number of detectors have been developed which recognize waveform characteristics either in the time domain (e.g. Liu & Fu 1983; Joswig & Schulte-Theis 1993) or using a time-frequency representation (e.g. Joswig 1990, 1995).

Waveform correlation has been applied to the classification of industrial seismicity (Israelsson 1990; Harris 1991) and to a lowering the detection threshold for anthropogenic events (e.g. Stevens et al. 2006; Gibbons & Ringdal 2010), earthquake clusters (e.g. Gibbons et al. 2007; Schaff 2010), microseismicity (Arrowsmith & Eisner 2006; Song et al. 2010), and evolving aftershock sequences (Yang et al. 2009; Peng & Zhao 2009; Harris & Dodge 2011). Correlation methods have been used increasingly and extensively in the identification of low frequency earthquakes (LFEs) in non-volcanic tremor, partly due to the difficulties in applying classical seismological methods to these signals (e.g. Shelly et al. 2007; Ohta & Ide 2011). The difficulty in identifying master events for template formation has led to the development of autocorrelation-based "blind" detectors for finding repeating signals in the absence of candidate events (Brown et al. 2008) and, more recently, Maceira et al. (2010) have applied subspace detectors, a higher dimensional generalization of correlation detectors (Harris 2006; Harris & Paik 2006), which permit greater waveform variability within clusters. There are increasing

efforts to incorporate correlation detectors into seismic processing pipelines (e.g. at the International Data Center for the Comprehensive Nuclear-Test-Ban Treaty in Vienna: Bobrov & Kitov 2011; Bobrov et al. 2011,) in order to facilitate more accurate and complete automatic event bulletins which exploit historical observations to a greater extent.

If $\boldsymbol{x}$ denotes a template waveform vector of N consecutive time-samples, normalized such that $\boldsymbol{x}.\boldsymbol{x} = 1$, then, if $\boldsymbol{y}(t)$ denotes the vector of N consecutive time-samples starting at time t, the correlation coefficient (CC)

$$C_{\boldsymbol{x}}(t) = \frac{\boldsymbol{x}.\boldsymbol{y}(t)}{\sqrt{\boldsymbol{y}(t).\boldsymbol{y}(t)}} \tag{1}$$

provides a fully normalized measure of similarity between the unit-norm template vector and the time-series beginning at time t. The significance of a CC value will depend upon of the complexity (time-bandwidth product) of the time-series (see, for example, Burnaby 1953). Indeed, other measures of waveform similarity such as phase cross-correlations (Schimmel 1999) and multitaper coherence (Prieto et al. 2009) are being applied increasingly for waveform realignment and cluster analysis. However, the CC value and related detection statistics remain the workhorse of large-scale calculations due to their simplicity and straightforward numerical implementation. The time-series in Eq. 1 is the ratio between two convolutions which are very efficiently evaluated using multiplication in the frequency domain.

While it is conceptually possible to estimate the relative location of events from correlation coefficients alone (Menke 1999), it has been demonstrated quite rigorously by Baisch et al. (2008) that very high CC values (> 0.95) are required to place formal constraints on hypocentral distance between "matching" events from single observations. Such high values are seldom observed, even between events known to be almost co-located (the CC value will be diminished by background noise even if the source-to-receiver Greens functions are essentially identical). Gibbons & Ringdal (2006) demonstrated correlation triggers with "low" CC values that were deemed to be plausible detections given that the local CC maximum exceeded by many times the standard deviation of the background level. That two events are almost co-located can be demonstrated if the time elapsed between template and detected signals is well-defined and identical at multiple stations in different directions, despite marginal CC values (e.g. Gibbons & Ringdal 2005). It is of course possible to set an absolute threshold for declaring detections on the CC-trace, although a more sensitive detector with fewer false alarms is more likely when considering the relation between the CC value at a given instant and typical values recorded at other times. Significant CC values can be detected using a power detector (e.g. Gibbons & Ringdal 2006; Schaff 2008) or by considering statistical outliers to the distribution of the CC-traces over long time intervals (e.g. Shelly et al. 2007). The second of these methods was deemed to be far more effective when considering events displaying significant variation in the source-time function,

since increased levels of the CC-traces can build up and decay over an interval of several seconds in contrast to the classical delta-function approximated when the source-time functions are very similar (Gibbons & Ringdal 2010).

For a given master event, the time separating the start of a signal template and the expected maximum of the CC-trace when a co-located event is detected is identical for all stations. This is the case whichever part of the wavetrain is selected for the signal template. Therefore, provided that the starting time of each CC-trace is corrected according to the starting time of the corresponding template, the CC-traces for all observing stations will attain their anticipated maxima simultaneously. This means that coherent array processing can be performed on the CC-traces over any receiver network to reduce the detection threshold for repeating signals (Gibbons & Ringdal 2006). Given that waveform similarity from sensor to sensor is not required, the CC-trace array processing can be performed over a sensor aperture which is, in principal, arbitrary. If events are not quite co-located then τ_{i1}, the travel-time from event 1 to station i will no longer equal τ_{i2}, the travel-time from event 2 to station i. If stations i and j are very close together, then $(\tau_{i2} - \tau_{i1})$ and $(\tau_{j2} - \tau_{j1})$ will be very similar, such that a zero move-out CC-trace stack is likely to interfere constructively at the time of best correlation. If sensors i and j are far apart, the decrease in waveform similarity resulting from the hypocentral distance will be compounded by significant changes to the path, and a greater difference between $(\tau_{i2} - \tau_{i1})$ and $(\tau_{j2} - \tau_{j1})$, such that the CC-traces at the different receivers may not stack constructively at zero-offset. Increasing the sensor aperture is likely to reduce the size of the geographical footprint in the source region over which multi-channel cross-correlation is effective. It may be desirable to process the single-channel CC-traces prior to stacking. For example, some authors (e.g. Vandecar & Crosson 1990) advocate applying the Fisher transformation (Fisher 1915) to map the correlation coefficient traces, bounded in the interval [-1:+1], to normally distributed functions. Selby (2010) applies the Fisher transform to the individual sensor CC-traces and applies the inverse Fisher transform to the zero-offset stack. Alternatively non-linear beamforming methods such as the Nth-root stack (McFadden et al. 1986) can be applied to provide increased weighting to times of high coherence, at the risk of introducing a degree of distortion to the stack.

Although the CC value is fully normalized, the properties of this and related detection statistic time-series may be affected significantly by contrasts in the waveform amplitudes within the template or the incoming data. For example, if correlating using a long waveform template, a relatively short high-amplitude signal in the incoming data will contribute significantly to the $\boldsymbol{y}(t).\boldsymbol{y}(t)$ term of Eq. 1, and relatively little to the $\boldsymbol{x}.\boldsymbol{y}(t)$ term, resulting in a lowering of CC values over an extended period. The envelope of the CC-trace will increase and decrease rapidly at times at which the short high amplitude signal overlaps only partially with the correlation window. Fig. 1 displays the correlation

between a 4 minute template, displaying a large variation in amplitudes, with a 15 minute data segment with no visible signals other than a very short duration wavetrain from a local event. The template contains both Pn and Sn arrivals and coda from a regional event, with Pn dominating on the vertical component and Sn on the horizontal components. The background level of both single channel and array stack CC-traces is reasonably stable over time until four minutes prior to the unrelated signal. Immediately after this time, the short signal in the incoming data stream contributes enormously to the denominator of the quotient in Eq. 1, but minimally to the numerator since the relatively small number of samples are being multiplied by the smallest amplitude part of the template wavetrain. Given the high amplitude of the short signal relative to the amplitudes of the background noise, the size of the denominator remains almost constant until the template passes the local signal. The amplitude of the numerator over this four minute interval varies almost proportionally to the amplitude of the time-reversed template waveform, resulting in CC-traces resembling mirror images of the template.

The significant dynamic range of the CC-trace over long time intervals presents a challenge to detection procedures, whether using power detectors or statistical outlier identification methods. It was recognized in the performance of surface wave tomography and calculations of Greens functions from correlations of ambient seismic noise that high-amplitude transients (e.g. from the presence of earthquake signals) were likely to bias the results and it became standard practice to perform so-called "one-bit correlations", only considering the sign of each sample (e.g. Campillo & Paul 2003; Larose et al. 2004; Shapiro et al. 2005). It was however noted by Sabra et al. (2005a) and Sabra et al. (2005b) that the one-bit clipping generated artificial high-frequency noise and modified the estimate of the ambient noise spectrum. They instead proposed a clipping threshold, determined for each station based upon a statistical analysis of background seismic noise over a timespan of a few days. The wavetrains available to us for forming signal templates for events at local, regional, and teleseismic distances are relatively transient with durations typically ranging from the order of a second to several minutes. This means that we are not at liberty to sacrifice the level of signal detail that the one-bit correlation procedure would demand. The clipping threshold strategy is also relatively high-risk given that the thresholds need to be specified carefully for each channel used. In addition, it was demonstrated by Gibbons et al. (2007) that waveform similarity can be sufficiently high for successful correlation detection over three orders of event magnitude (with a corresponding range of waveform amplitudes). We would want to set the clipping threshold sufficiently high to prevent waveform distortion of signals that could be valid detections from the chosen template, and yet this threshold may still not be low enough to prevent an unwanted modulation due to an exceptional transient as seen in Fig. 1.

In this paper, we advocate a slightly different procedure whereby the correlation is performed on waveforms with reduced dynamic range but which resemble the original seismograms locally. A

straightforward way to generate such surrogate waveforms is to scale the original seismogram by a trace comprising a pointwise moving estimate of the envelope amplitude, averaged over the length scale over which the optimal match with the original seismogram is required. The simplest measure of the envelope is a mean of the absolute values and we denote the rescaled traces Ratio-to-Moving-Average (or RMA) seismograms. In Sec. 2 we demonstrate a successful correlation detection of a repeating seismic signal and demonstrate how the detection can be missed by the influence of a foreign signal with high amplitudes. In Sec. 3, the concept of the RMA-trace is explained together with an illustration of how the procedure would have mitigated the failure of the example in the previous section. A correlation calculation on a data segment from the extensive aftershock sequence of a large earthquake is described in Sec. 4 together with a demonstration of how the RMA procedure appears to improve the likelihood of identifying events closely related to the master event.

2 IMPLEMENTATION AND PERFORMANCE OF CORRELATION DETECTORS

Fig. 2 illustrates the complete multi-channel correlation detection process for which a detection has been declared. The waveform template is the signal from the Indian underground nuclear test in 1974, recorded on the NORSAR array at a distance of 52.5 degrees. Waveforms at the time of a selected master event signal are bandpass filtered into a frequency band providing an optimal signal-to-noise ratio (SNR) and optimizing the likelihood of detecting subsequent events at the site of interest. For the example displayed here, a 1.2-3.2 Hz band was chosen omitting both the lowest frequencies (likely to display a lower SNR for a smaller event) and the highest frequencies (which may limit the geographical source footprint too greatly). The length of waveform template providing optimal detectability varies also considerably according to the properties of the signal being observed; in principle, the longest possible template is desirable to maximise the time-bandwidth product. In practice, a cut-off point is required to omit parts of the wavetrain which, from SNR considerations, are likely to degrade detector performance. The red waveforms in Fig. 2 illustrate a 30 second long template for the teleseismic Indian nuclear test signal. For simplicity, a uniform window has been taken for all sites of the array, ignoring time-delays over the array aperture.

It is illustrated in Fig. 2 how different the short period waveforms are on different sites of the array (see Bungum & Husebye 1971) and also how greatly the amplitude of the initial arrival varies (see Ringdal & Husebye 1982). The template is correlated sample by sample with an incoming data stream on May 18, 1998, resulting in the single channel CC-traces (blue). There is a convincing ripple-for-ripple match between the 1974 and 1998 signals on each sensor, although the characteristics of the corresponding CC-traces vary according to the waveform properties. The uppermost of the blue traces (NC200_sz CC) displays a degree of "ringing": significant sidelobes resulting from the simplicity of

the waveform. Although the signal at site NAO01 has a far lower amplitude than at NC200, the signal complexity appears somewhat greater and the resulting CC-trace (lowermost blue trace in Fig. 2) is closer to the ideal delta function. Local maxima of the single channel CC-traces appear to align well and they stack constructively to form a peak significantly above the background level: a convincing correlation detection.

Just as the detection threshold can be reduced using array processing, the validity of detections can be assessed by measuring the alignment of the single-channel CC-traces. For an array of moderate aperture, i.e. such that the receiver-to-source backazimuth is comparable for all sensors, frequency-wavenumber (f-k) analysis can be performed on the ensemble of individual CC-traces to expose clear false alarms automatically (Gibbons & Ringdal 2006). Specifically, a reasonable correlation between a wavefront propagating with slowness vector $\boldsymbol{s}_1$ and one propagating with slowness vector $\boldsymbol{s}_2$ will approximate a wavefront propagating over the same aperture with a slowness vector $(\boldsymbol{s}_2 - \boldsymbol{s}_1)$. CC-traces which indicate a propagating plane wave with a non-zero slowness vector can therefore not possibly be the result of a correlation between two arrivals from the same direction. (For example, Gibbons & Ringdal 2012, used waveform correlation to monitor events at the North Korea nuclear test site using the MJAR array in Japan and, over a three year period, found that this type of f-k post-processing reduced the number of candidate detections from 2496 to 7.)

The slowness grid in Fig. 2 indicates a clearly defined zero slowness-vector as is required for the f-k post-processing test of Gibbons & Ringdal (2006). This is to say that the array is unable to resolve any difference between the paths travelled by the two wavefronts. It is noted that the array aperture over which the f-k post-processing is valid is larger than that over which coherent f-k analysis for the actual waveforms is valid, since the condition of waveform similarity is from event to event and not sensor to sensor. In addition, the significant deviations in backazimuths observed due to heterogeneities below the array (e.g. Berteussen 1976) do not influence the validity of the CC-trace f-k analysis since they are caused by path and site effects which are almost identical for the correlating signals and cancel in the correlation operation.

Fig. 3 displays the attempt to detect the 1998 Indian nuclear test shown in Fig. 2 but under a scenario whereby a large amplitude signal from an unrelated event arrives at the array many seconds after the peak amplitudes of the nuclear test signal. An STA/LTA detector on a beam directed towards the predicted slowness vector, followed by classical slowness analysis of the detected signal, would detect the test signal and classify it correctly without difficulty. The amplitude of the Japan earthquake signal, added to the 1998 data segment with no scaling applied, exceeds the amplitude of the Indian explosion signal by an order of magnitude or more. As for the India signal, the amplitude of the Japan signal varies substantially from sensor to sensor of the array although with very different amplitude

ratios. The correlation with the 30 second template fails to detect the nuclear test signal despite the characteristic P-arrival, with the highest amplitudes, being clearly visible. The initial arrival from Japan, correlating with the lowest amplitude parts of the template waveform, diminishes the CC value at the predicted time for the reasons illustrated in Fig. 1. On the single channel CC-traces there is not even a local maximum at the time indicated in the absence of the embedded signal, although the zero move-out summation suppresses amplitudes with a different alignment resulting in a low local maximum at the correct time on the stack. However, the f-k analysis produces no evidence of a convincing zero slowness vector.

Shortening the template in Fig. 3 sufficiently may have avoided the failure displayed here, but would provide a master waveform with a lower time-bandwidth product with consequences for the detector performance. Similarly, a data glitch at the time of the P-arrival, rather than an intrusive signal several seconds after P, would mean that the lower amplitude P-coda would be the only data available for detecting nuclear test signal. A framework whereby templates are split, to prevent a very short high SNR signal from dominating the detection statistic, is conceivable but would also require some rather arbitrary parameters (e.g. how many segments would the template be broken into?), and would increase the complexity (and reduce the efficiency) of the process greatly.

3 DEFINITION OF RMA SEISMOGRAMS

We argue in this paper that more robust correlation detectors can be achieved by replacing seismograms with traces where the value at every sample is divided by a scaling factor approximately proportional to some measure of a characteristic signal amplitude within a time-window centered on that sample. The nature of the rescaled traces will be determined by the length of the window used to estimate the characteristic amplitude, of which the simplest estimate is a moving average of the absolute values. The extreme case is of a window length of a single sample. This will result in samples that are either plus or minus unity: the one-bit seismogram. A very long window will result in a scaling factor which varies very slowly with time and so maintaining an envelope shape that is similar to that of the original seismogram over the length scale of the window for averaging. We seek an averaging window length that is short relative to the template window length, but long enough to contain many zero crossings in the frequency band being examined, such that the peak-to-peak amplitude ratios that define the characteristic waveform signature are preserved.

The upper two traces of Fig. 4 display bandpass filtered waveforms on the NORSAR array from an earthquake at a distance of about 4 degrees. Although the separation between the sites is small compared with the epicentral distance, the characteristics of the waveforms differ dramatically. The Pn phase at site NBO03 is very impulsive (a three figure SNR) whereas that at site NC302 is very

emergent (a single figure SNR). The Sn phase at NBO03 is also far clearer than that at NC302. Under the waveforms are the corresponding STA traces, where the value at each sample is the mean of the absolute values over a six second window centered on the time of that sample. The STA traces vary relatively smoothly with the only rapid changes related to the very impulsive arrival. The level of these moving average traces is significantly below the maximum amplitudes observed. The definition of this trace of scaling factors is of course arbitrary; it is only the intention that it represents some measure of a representative amplitude in a moving window. It is possible to generate traces that more closely resemble the signal envelope although these will vary more rapidly, depending on the fidelity required. The smoothness of the moving window mean traces is a desirable property since we do not wish the dynamic range of scaled seismograms to vary more rapidly than the original traces. The lower two traces in the main panel of Fig. 4 show the corresponding RMA seismograms which appear to be relatively featureless with only the most impulsive seismic arrivals being visible. Otherwise, there is little in the RMA traces that differentiates signal from noise. The small inset panel of Fig. 4 displays a six second long segment of a filtered seismogram together with the corresponding RMA trace. There is a very close correspondence between waveform features.

In Fig. 5 we revisit our attempt to detect the signal from the 1998 Indian nuclear test with correlation using the 1974 template, demonstrated to fail in Fig. 3 when a high amplitude signal from an unrelated earthquake arrives shortly after the start of the nuclear test signal. The waveforms are band-pass filtered initially as before, although this time we also calculate the moving average and RMA traces prior to the correlation. As with the RMA waveforms in Fig. 4, the corresponding traces in Fig. 5 are relatively featureless with little difference between the preceding noise and the signal. Only the P-arrivals from the nuclear test signal stand out; the more emergent, albeit larger amplitude, signal from Japan is not clearly identifiable.

The uppermost trace in Fig. 5, the array CC-trace, has a clear peak at the same time as that displayed in Fig. 2. Being many times greater than the standard deviation of the background values of this trace, this signal would be identified readily. The single channel CC-traces are notably poorer than those displayed in Fig. 2. This is only to be expected given the significantly shorter part of the Indian test signal now present in the incoming data. The Japan signal, with amplitudes an order of magnitude greater than the India signal, still dominates those parts of the time-series where there is overlap. However, the rescaling has diminished the influence of this part of the waveform in the correlation coefficient. Given the rather constant level of the RMA seismograms, it can be assumed that the contribution to the CC value of a given part of the correlating window is approximately proportional to the relevant fraction of the window length. In this sense, the results are likely to resemble those obtained using the split-window idea mentioned before, but without the arbitrarily chosen parameters

and additional complexity of the code. Significantly, the f-k grid in Fig. 5 provides a clear indication of a zero slowness vector.

4 AN EXAMPLE FROM AN AFTERSHOCK SEQUENCE

Aftershock sequences following major earthquakes can generate thousands of events in rapid succession which can overwhelm analyst resources in the days following the main event. Harris & Dodge (2011) demonstrate how the situation can be ameliorated using correlation methods automatically to classify very closely related events into clusters for more efficient characterization. The top trace of Fig. 6 displays an hour of data from the center element of the Karatau array (KKAR) in southern Kazakhstan some 14 hours after the magnitude 7.6, 2005 October 8, Kashmir earthquake. The amplitudes are dominated by three or four large events although the clipped trace displayed underneath reveals that the KKAR data for this hour contains signal after signal from events in the sequence. We note that very many of the arrivals (both P and S) are very impulsive at KKAR with the largest amplitudes usually occurring with the direct phase arrival.

A template is extracted from a well-located aftershock some 90 minutes after the main event, displayed in red at the top of Fig. 6. The correlation coefficient trace for this single station is displayed in the third trace from the top and it is clear that the trace contains peak after peak, some of which appear to be well-defined and others that rise clearly above the background level, but which do not resemble the classic delta-function correlation peak. The blue trace is the array CC-trace which has significantly fewer peaks than the single channel CC-trace, a strong indication that many such peaks are likely to be spurious. While there are fewer detections on the array CC-trace, the setting of detection thresholds still appears to be problematic.

The only one of these peaks that corresponds to an event which is in clear proximity to the master event occurs at about 19:10 UT (the USGS specification for this event is magnitude 4.9, 34.80°N, 73.17°E, depth 10 km at a time 19.08.00). We can build confidence in the quality of this correlation detection in that correlations between the signals from this event and the master event are highly convincing at many different stations in different directions from the source. The peak on the single channel CC-trace at this time is visible but is not one of the greatest peaks in this time interval. Not until the array CC-stack is formed, does this peak really become significant compared with the surrounding values. There are numerous other peaks in the array CC-stack, all of which correspond to "real" events in the sequence, although many such detections are unique to this array. The relatively small aperture of the KKAR results in a number of detections which pass the f-k post-processing criteria due to the similarity between the directions of arrival at this particular station. It is yet to be seen as to whether such detections are very useful in an automatic classification system such as that proposed by Harris

& Dodge (2011). If attempting to match the waveforms from these events at stations with different backazimuths fails, it may mean that any association with the master event may be spurious.

The lower panel of Fig. 6 displays the equivalent traces when the waveforms have been replaced by the rescaled RMA traces. The filtered waveforms have a very large dynamic range and have (as seen in Fig. 4) been replaced by seismograms which are relatively featureless except for the occasional spike caused by a local amplitude spike of shorter duration than the averaging window. The peak at 19:10 is clear on the single channel CC-trace and is in fact the only clear detection in this interval. The large dynamic range of the single channel CC-trace in the upper panel has been replaced by a function with an almost constant envelope. In the RMA array CC-trace (the lowermost trace in Fig. 6), the variability is suppressed further. There are arguably three clear detections, the validity of which needs to be determined by f-k post-processing at KKAR and ultimately cross-validation with recordings at other stations. There are clear differences between the array CC-trace stacks with and without the RMA procedure being applied, particularly with respect to the setting of a robust detection threshold. Caution needs to be applied if detections result from correlating the filtered waveforms which are not made when correlating the RMA waveforms.

5 CONCLUSIONS

We have demonstrated situations in which the performance of waveform correlation detectors is degraded as a the result of large changes in the amplitudes on seismograms. Detections are usually made by identifying outliers to the distribution of values in traces of correlation coefficients or related detection statistics. Transient high-amplitude signals will result in a significant modulation of these CC-traces which make it difficult to set robust detection thresholds. Correlation detectors may fail to detect a signal clearly visible in the data if an unrelated signal falls within the time interval spanned by the template. In extensive aftershock sequences, CC-traces may be modulated heavily due to changes in the waveform amplitudes, possibly resulting in numerous false detections and missed genuine detections.

We have demonstrated that dividing each sample of a waveform by a moving average of absolute values of the original seismogram results in a time-series, which we denote an RMA-seismogram. This scaled trace is largely featureless over long time-windows but resembles the original waveforms closely, ripple-for-ripple, over shorter time windows. For the frequencies typically used in regional and teleseismic seismology (1-10 Hz) we have used a window length of 6 seconds for calculating the moving average trace. The properties of the RMA-seismograms will differ according to the dominant frequency of the waveform and the length of the moving average window. Correlators on the RMA traces appear to perform more robustly providing convincing detections where they are missed using

the bandpass filtered waveforms alone and reducing the number of false detections which are artefacts of the convolving of two time-series containing high amplitudes. The division by the moving average traces is a pre-processing step only and does not effect the algorithms used to perform the correlations. It is therefore straightforward to compare the performance of detectors with original seismograms and RMA-seismograms with diverse parameters.

ACKNOWLEDGMENTS

This work was supported by the Air Force Research Laboratory under contract number FA9453-11-C-0230.

We are grateful to the Kazakh National Data Center for permission to use data from the KKAR array and to Terri McDonald Hauk for preparation of this data.

All remaining data is courtesy of the Norwegian National Data Center at NORSAR and is openly available from

`http://www.norsardata.no/NDC/data/autodrm.html`

REFERENCES

Allen, R., 1982, Automatic phase pickers: Their present use and future prospects, *Bull. Seism. Soc. Am.*, **72**(6B), S225–S242.

Allen, R. V., 1978, Automatic earthquake recognition and timing from single traces, *Bull. Seism. Soc. Am.*, **68**(5), 1521–1532.

Arrowsmith, S. J. & Eisner, L., 2006, A technique for identifying microseismic multiplets and application to the Valhall field, North Sea, *Geophysics*, **71**(2), V31–V40.

Baisch, S., Ceranna, L., & Harjes, H.-P., 2008, Earthquake Cluster: What Can We Learn from Waveform Similarity?, *Bull. Seism. Soc. Am.*, **98**(6), 2806–2814.

Berteussen, K. A., 1976, The origin of slowness and azimuth anomalies at large arrays, *Bull. Seism. Soc. Am.*, **66**, 719–741.

Bobrov, D., Kitov, I., & Zerbo, L., 2011, Perspectives of cross correlation in seismic monitoring at the International Data Centre, Preprint posted on http://arxiv.org/abs/1112.4696.

Bobrov, D. I. & Kitov, I. O., 2011, Analysis of the 2008 Chinese Earthquake Aftershocks Using Cross-Correlation, in *Proceedings of the 2011 Monitoring Research Review: "Ground-Based Nuclear Monitoring Technologies", Tucson, Arizona, Sept 13-15, 2011 LA-UR-11-04823*, pp. 811–821 (Paper 06–01).

Brown, J. R., Beroza, G. C., & Shelly, D. R., 2008, An autocorrelation method to detect low frequency earthquakes within tremor, *Geophysical Research Letters*, **35**(16), L16305+.

Bungum, H. & Husebye, E. S., 1971, Errors in time delay measurements, *Pure appl. geophys.*, **91**, 56–70.

Burnaby, T. P., 1953, A Suggested Alternative to the Correlation Coefficient for testing the Significance of

Agreement between Pairs of Time Series, and its Application to Geological Data, *Nature*, **172**(4370), 210–211.

Campillo, M. & Paul, A., 2003, Long-Range Correlations in the Diffuse Seismic Coda, *Science*, **299**(5606), 547–549.

Fisher, R. A., 1915, Frequency distribution of the values of the correlation coefficients in samples from an indefinitely large population, *Biometrika*, **10**(4), 507–521.

Geller, R. J. & Mueller, C. S., 1980, Four Similar Earthquakes in Central California, *Geophysical Research Letters*, **7**(10), 821–824.

Gibbons, S. J. & Ringdal, F., 2005, Detection of the aftershock from the 16 August 1997 Kara Sea event using waveform correlation, Tech. rep., NORSAR, Kjeller, Norway.

Gibbons, S. J. & Ringdal, F., 2006, The detection of low magnitude seismic events using array-based waveform correlation, *Geophys. J. Int.*, **165**, 149–166, doi: 10.1111/j.1365-246X.2006.02865.x.

Gibbons, S. J. & Ringdal, F., 2010, Detection and Analysis of Near-Surface Explosions on the Kola Peninsula, *Pure and Applied Geophysics*, **167**(4), 413–436.

Gibbons, S. J. & Ringdal, F., 2012, Seismic Monitoring of the North Korea Nuclear Test Site Using A Multi-Channel Correlation Detector, *IEEE Trans. Geoscience and Remote Sensing*, In press, doi: 10.1109/TGRS.2011.2170429.

Gibbons, S. J., Bøttger Sørensen, M., Harris, D. B., & Ringdal, F., 2007, The detection and location of low magnitude earthquakes in northern Norway using multi-channel waveform correlation at regional distances, *Physics of the Earth and Planetary Interiors*, **160**(3-4), 285–309, doi: 10.1016/j.pepi.2006.11.008.

Harris, D. B., 1991, A waveform correlation method for identifying quarry explosions, *Bull. Seism. Soc. Am.*, **81**, 2395–2418.

Harris, D. B., 2006, Subspace Detectors: Theory, Tech. rep., UCRL-TR-222758, Lawrence Livermore National Laboratory.

Harris, D. B. & Dodge, D. A., 2011, An autonomous system for grouping events in a developing aftershock sequence, *Bull. Seism. Soc. Am.*, **101**, 763–774.

Harris, D. B. & Paik, T., 2006, Subspace Detectors: Efficient Implementation, Tech. rep., UCRL-TR-223177, Lawrence Livermore National Laboratory.

Israelsson, H., 1990, Correlation of waveforms from closely spaced regional events, *Bull. Seism. Soc. Am.*, **80**(6B), 2177–2193.

Joswig, M., 1990, Pattern recognition for earthquake detection, *Bull. Seism. Soc. Am.*, **80**(1), 170–186.

Joswig, M., 1995, Automated classification of local earthquake data in the BUG small array, *Geophys. J. Int.*, **120**(2), 262–286.

Joswig, M. & Schulte-Theis, H., 1993, Master-event correlations of weak local earthquakes by dynamic waveform matching, *Geophys. J. Int.*, **113**, 562–574.

Larose, E., Derode, A., Campillo, M., & Fink, M., 2004, Imaging from one-bit correlations of wideband diffuse wave fields, *J. Appl. Phys.*, **95**, 8393–8399.

Liu, H.-H. & Fu, K.-S., 1983, An Application of Syntactic Pattern Recognition to Seismic Discrimination, *Geoscience and Remote Sensing, IEEE Transactions on*, **GE-21**(2), 125–132.

Maceira, M., Rowe, C. A., Beroza, G., & Anderson, D., 2010, Identification of low-frequency earthquakes in non-volcanic tremor using the subspace detector method, *Geophysical Research Letters*, **37**(6), L06303+.

McFadden, P. L., Drummond, B. J., & Kravis, S., 1986, The Nth-root stack; theory, applications, and examples, *Geophysics*, **51**(10), 1879–1892.

Menke, W., 1999, Using waveform similarity to constrain earthquake locations, *Bull. Seism. Soc. Am.*, **89**(4), 1143–1146.

Ohta, K. & Ide, S., 2011, Precise hypocenter distribution of deep low-frequency earthquakes and its relationship to the local geometry of the subducting plate in the Nankai subduction zone, Japan, *Journal of Geophysical Research*, **116**(B1), B01308+.

Peng, Z. & Zhao, P., 2009, Migration of early aftershocks following the 2004 Parkfield earthquake, *Nature Geoscience*, **2**(12), 877–881.

Prieto, G. A., Parker, R. L., & Vernon, F. L., 2009, A Fortran 90 library for multitaper spectrum analysis, *Computers & Geosciences*, **35**(8), 1701–1710, doi: 10.1016/j.cageo.2008.06.007.

Ringdal, F. & Husebye, E. S., 1982, Application of Arrays in the Detection, Location, and Identification of Seismic Events, *Bull. Seism. Soc. Am.*, **72**, S201–S224.

Sabra, K. G., Gerstoft, P., Roux, P., Kuperman, W. A., & Fehler, M. C., 2005, Surface wave tomography from microseisms in Southern California, *Geophysical Research Letters*, **32**(14), L14311+.

Sabra, K. G., Gerstoft, P., Roux, P., Kuperman, W. A., & Fehler, M. C., 2005, Extracting time-domain Green's function estimates from ambient seismic noise, *Geophysical Research Letters*, **32**(3), L03310+.

Schaff, D., 2010, Improvements to detection capability by cross-correlating for similar events: a case study of the 1999 Xiuyan, China, sequence and synthetic sensitivity tests, *Geophys. J. Int.*, **180**, 829–846.

Schaff, D. P., 2008, Semiempirical Statistics of Correlation-Detector Performance, *Bull. Seism. Soc. Am.*, **98**(3), 1495–1507.

Schimmel, M., 1999, Phase cross-correlations: Design, comparisons, and applications, *Bull. Seism. Soc. Am.*, **89**(5), 1366–1378.

Selby, N. D., 2010, Relative Locations of the October 2006 and May 2009 DPRK Announced Nuclear Tests Using International Monitoring System Seismometer Arrays, *Bull. Seism. Soc. Am.*, **100**(4), 1779–1784.

Shapiro, N. M., Campillo, M., Stehly, L., & Ritzwoller, M. H., 2005, High-Resolution Surface-Wave Tomography from Ambient Seismic Noise, *Science*, **307**(5715), 1615–1618.

Shelly, D. R., Beroza, G. C., & Ide, S., 2007, Non-volcanic tremor and low-frequency earthquake swarms, *Nature*, **446**(7133), 305–307.

Song, F., Kuleli, H. S., Toksoz, M. N., Ay, E., & Zhang, H., 2010, An improved method for hydrofracture-induced microseismic event detection and phase picking, *Geophysics*, **75**(6), A47–52.

Stevens, J. L., Gibbons, S., Rimer, N., Xu, H., Lindholm, C., Ringdal, F., Kvaerna, T., & Murphy, J. R., 2006, Analysis and simulation of chemical explosions in nonspherical cavities in granite, *Journal of Geophysical*

Research - Solid Earth, **111**(B4), B04306+.

Vandecar, J. C. & Crosson, R. S., 1990, Determination of teleseismic relative phase arrival times using multi-channel cross-correlation and least squares, *Bull. Seism. Soc. Am.*, **80**(1), 150–169.

Withers, M., Aster, R., Young, C., Beiriger, J., Harris, M., Moore, S., & Trujillo, J., 1998, A comparison of select trigger algorithms for automated global seismic phase and event detection, *Bull. Seism. Soc. Am.*, **88**(1), 95–106.

Yang, H., Zhu, L., & Chu, R., 2009, Fault-Plane Determination of the 18 April 2008 Mount Carmel, Illinois, Earthquake by Detecting and Relocating Aftershocks, *Bull. Seism. Soc. Am.*, **99**(6), 3413–3420.

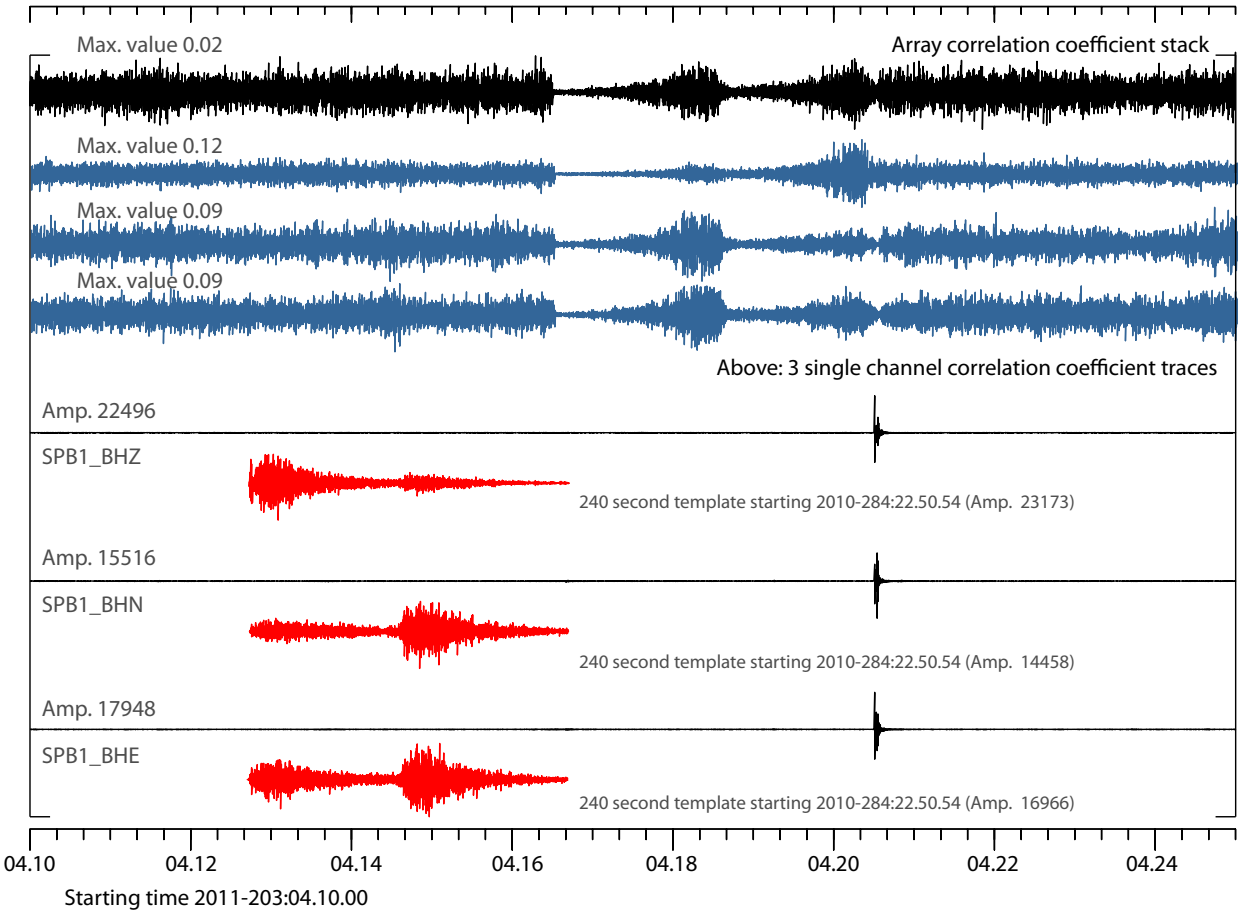

Figure 1. Correlation on the SPITS array of a 240 second long waveform template from an earthquake on Novaya Zemlya at a distance 1135 km with a 15 minute long data segment containing a large amplitude signal from a local event. All waveforms are bandpass filtered 2.0-8.0 Hz prior to template extraction and correlation. The array correlation stack is formed using 21 broadband channels: 9 vertical, 6 East-West and 6 North-South.

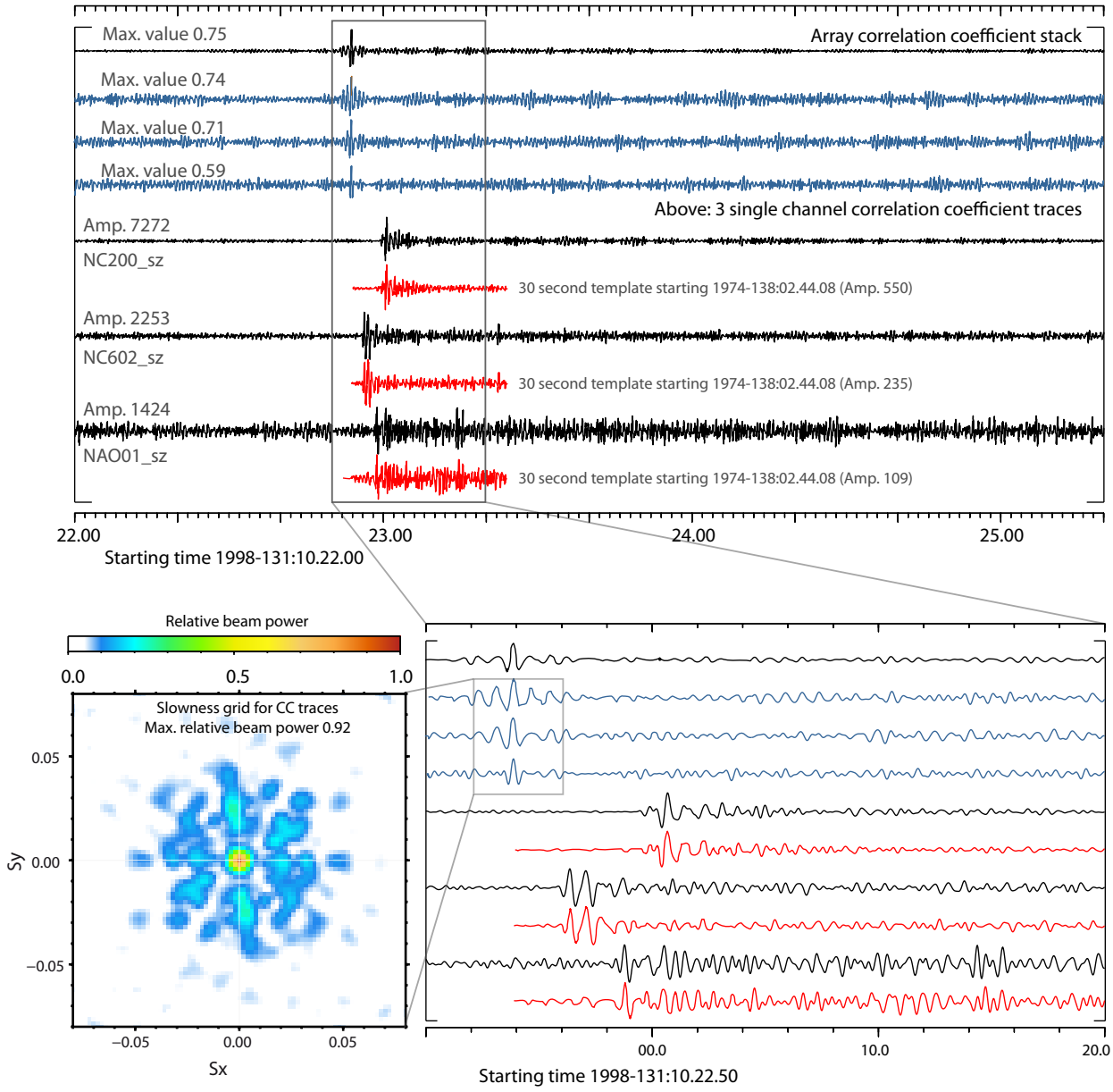

Figure 2. Detection using waveform correlation on the NORSAR array of the signal from the May 11, 1998, *Shakti* nuclear test at the Pokhran site in India using the May 18, 1974, *Smiling Buddha* test signal as a template. All waveforms are bandpass filtered 1.2-3.2 Hz prior to template extraction and correlation. The array correlation stack is formed using 34 of the short period vertical channels. The 30 second template starting at 1974-138:02.44.08 attains a maximum correlation coefficient of 0.75 at a time 1998-131:10.22.53.86. The template waveform is displayed aligned according to the time of the correlation maximum. The f-k spectrum of the single channel correlation coefficient traces is formed using a 2 second long data window centered at the time of the local maximum on the array stack. Note that the 1974 and 1998 recordings are made on different sensors with slightly different instrument responses and are not corrected. No comparison should therefore be made between the amplitudes for the 1974 and 1998 signals.

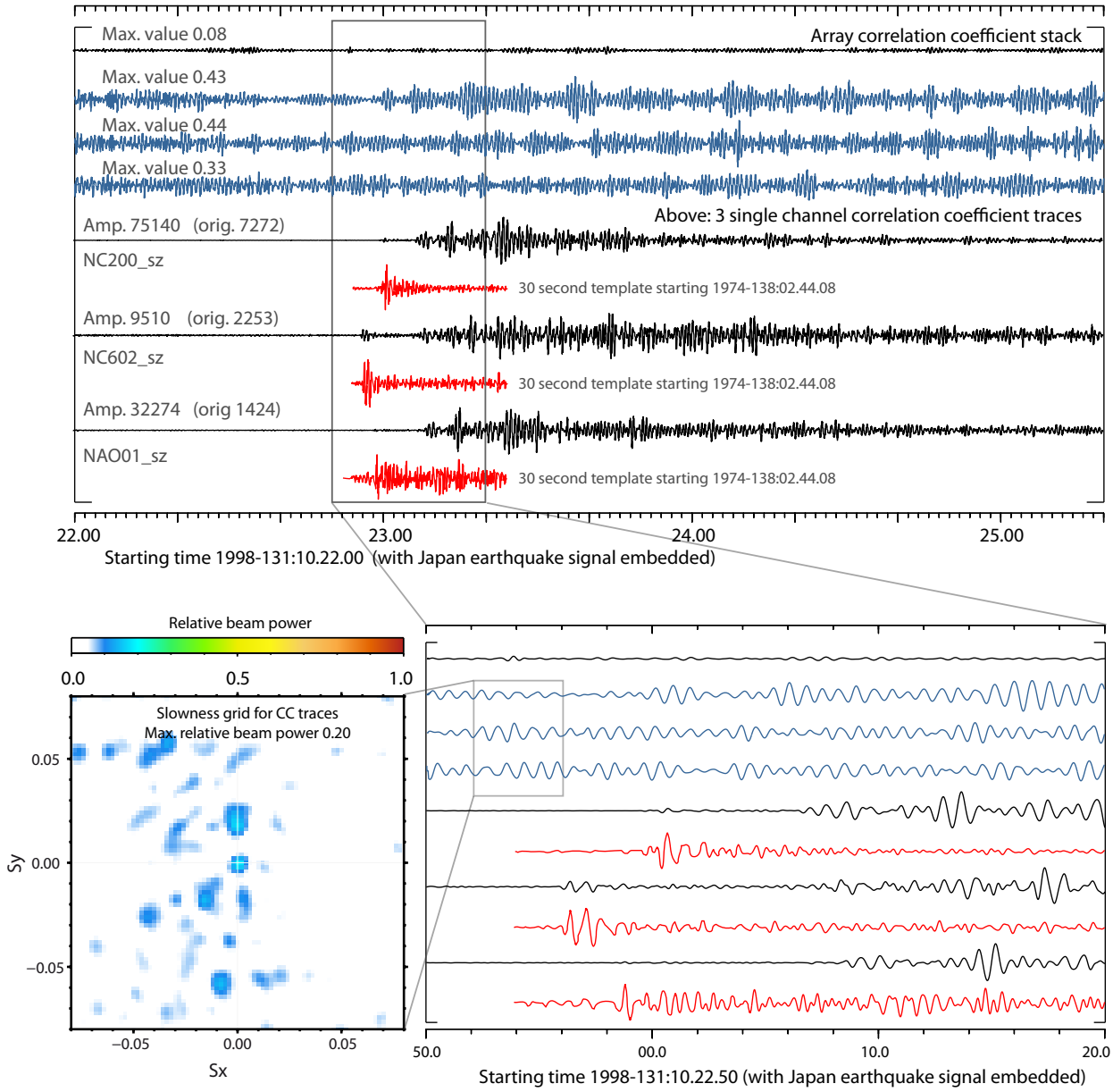

Figure 3. Identical to Fig. 2 except that a foreign signal (starting time 2011-068:02.56.48) has been submerged into the data stream at a time 1998-131:10.23.05 prior to the correlation procedure. The submerged signal results from an earthquake near the East Coast of Honshu, Japan, which the United States Geological Survey (USGS: http://earthquake.usgs.gov/) has specified as magnitude 7.2 at 38.424°N, 142.836°E, 32 km deep at a time 02.45.20 on 9 March 2011. The template waveforms are displayed with the same alignment as in Fig. 2 despite the correlation coefficient trace stack not having a maximum at this time. The f-k spectrum is calculated on the same time-window as in Fig. 2.

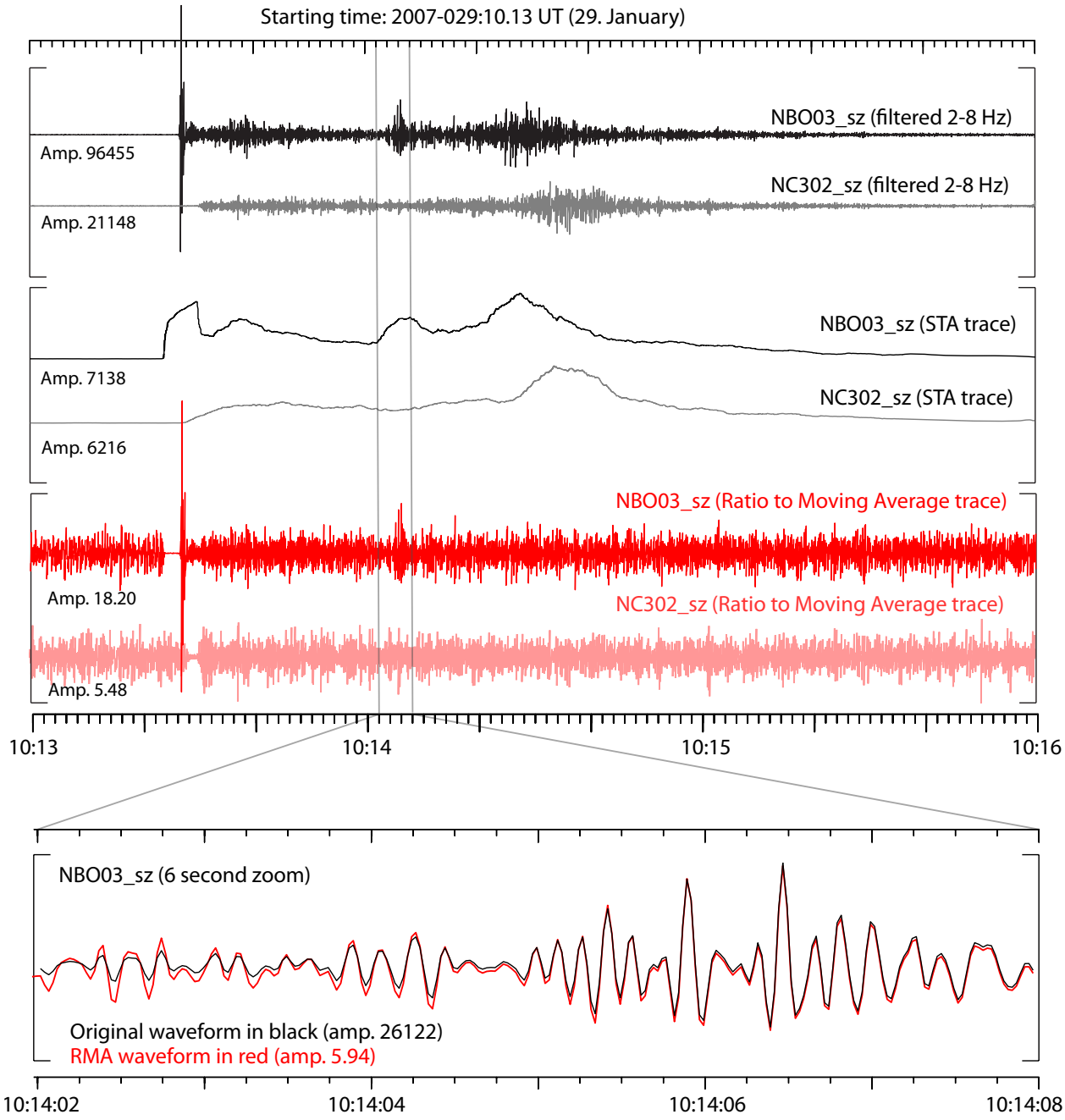

Figure 4. Generation of Ratio-to-Moving-Average (RMA) seismograms. In the top panel, the uppermost two traces display bandpass filtered waveforms on two sites of the large-aperture NORSAR array from a single earthquake off the western coast of Norway. The central two traces display STA traces constructed with a 0.025 second sampling interval where each sample gives a mean of absolute values over a 6 second interval. The lowermost two traces (red) display the RMA traces: the bandpass filtered waveforms divided by the STA traces. The lower panel displays a 6 second long zoom of an original waveform and an RMA trace superimposed.

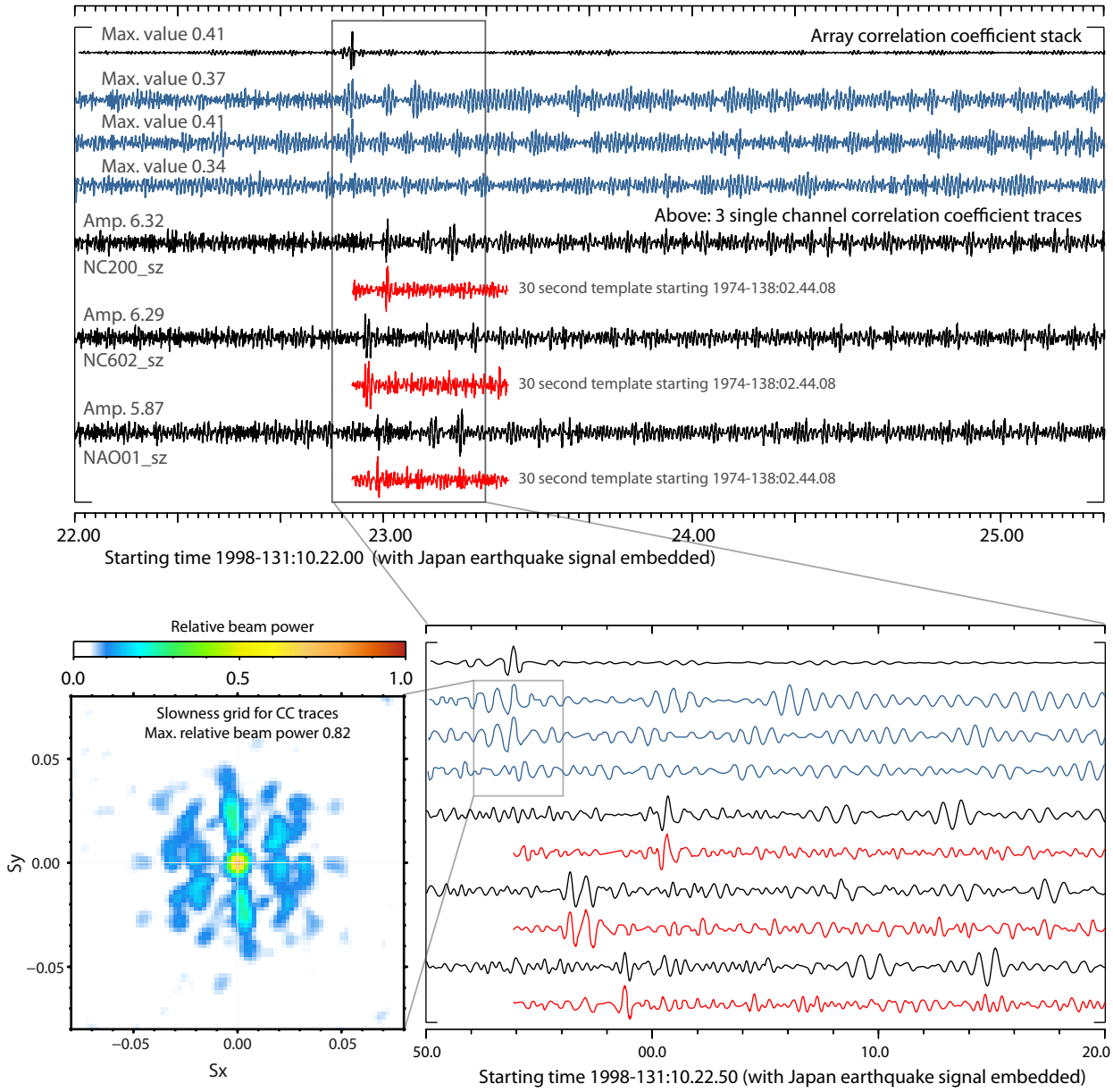

Figure 5. Identical to Fig. 3 except that the original waveforms have been replaced with the RMA seismograms prepared as demonstrated in Fig. 4.

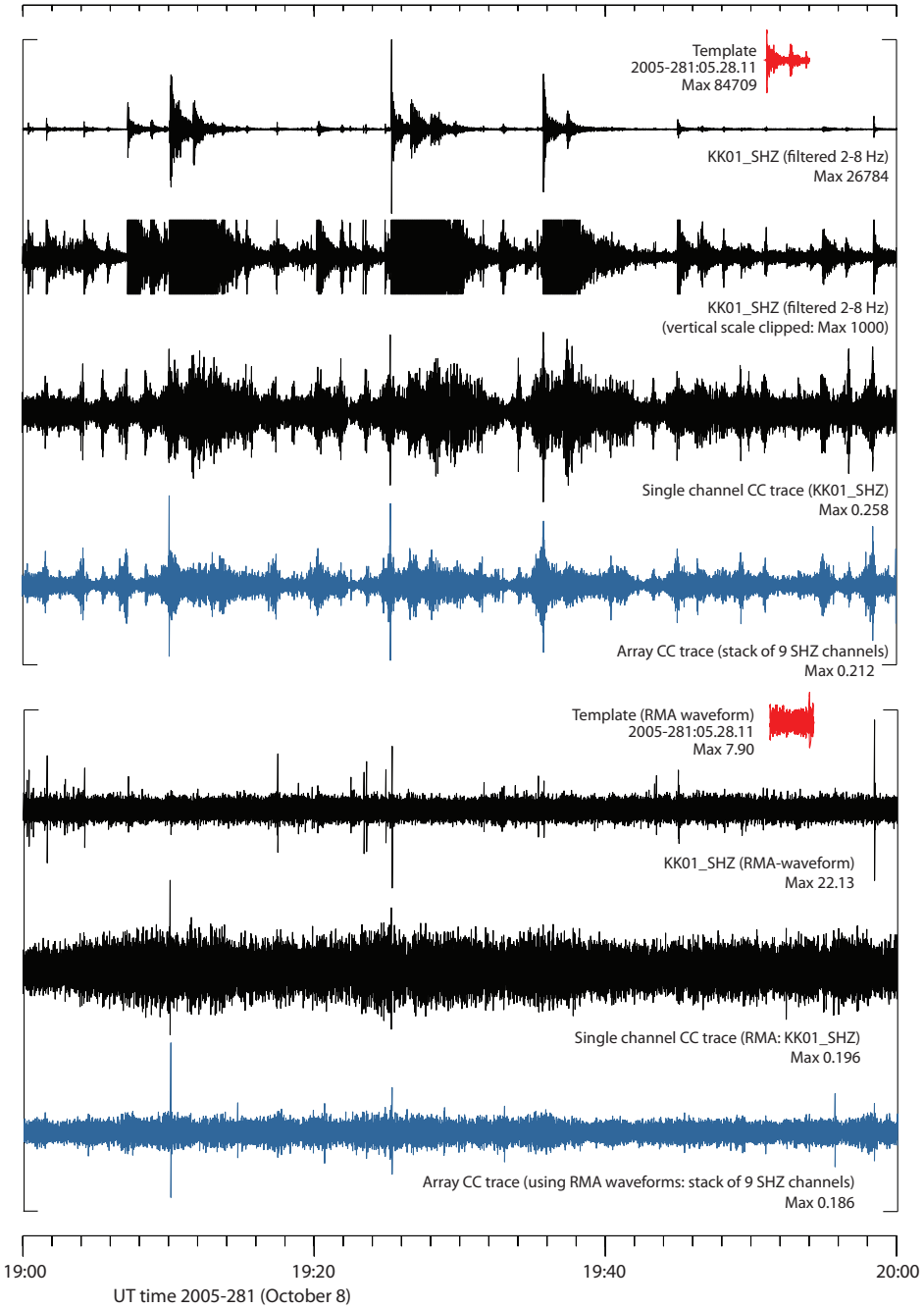

Figure 6. A search through one hour of data from the KKAR 9-element array in southern Kazakhstan for repeating aftershocks following the magnitude 7.6 Kashmir earthquake October 8, 2005, at a distance of approximately 9 degrees. A template is taken from a single aftershock, located by USGS at 34.76°N, 73.15°E, depth 10 km at a time 05.26.05. The upper frame shows the waveforms and corresponding detection statistic traces when the only pre-processing is bandpass filtering. The lower frame shows the corresponding traces when the filtering is followed by a calculation of the RMA for both template and incoming data. In this segment, only a single detection shortly after 19:10 UT can be unequivocally associated with an event located in the immediate vicinity of the master event. When the correlation procedure is applied to the filtered waveforms alone, this detection is not significantly above the background noise for the single channel case. Note the reduced dynamic range for the detection statistic traces as well as the waveforms for the RMA case in the lower frame.